

# AdS boson stars in string theory

Alex Buchel

*Department of Applied Mathematics, Department of Physics and Astronomy,  
University of Western Ontario  
London, Ontario N6A 5B7, Canada;  
Perimeter Institute for Theoretical Physics  
Waterloo, Ontario N2J 2W9, Canada*

## Abstract

Boson stars are stationary soliton-like gravitational configurations supported by a complex scalar field charged under the global  $U(1)$  symmetry. We discuss properties of boson stars in type IIB supergravity approximation to string theory. A notable difference is that in supergravity models the global symmetry of the complex scalar field is gauged. We focus on global asymptotically  $AdS_5$  space-time, where the boson stars are expected to represent stable low-energy non-thermal excitations in holographically dual quiver conformal gauge theory.

October 27, 2015

# Contents

<b>1</b>	<b>Introduction</b>	<b>2</b>
<b>2</b>	<b>Quiver <math>\mathcal{N} = 1</math> supersymmetric CFT holography</b>	<b>3</b>
2.1	GHPT effective action . . . . .	3
2.2	Thermal state without scalar condensates in microcanonical ensemble .	4
2.3	Thermal states with scalar condensate in microcanonical ensemble . . .	7
<b>3</b>	<b>Boson stars in a toy model</b>	<b>11</b>
<b>4</b>	<b>Boson stars in supergravity</b>	<b>14</b>
<b>5</b>	<b>Conclusion</b>	<b>19</b>

## 1 Introduction

Consider an effective gravitational action containing Einstein-Hilbert term and a complex scalar field  $\Psi$  with an exact global  $U(1)$  symmetry,

$$S_{d+1} = \frac{1}{16\pi G_{d+1}} \int_{\mathcal{M}_{d+1}} dx^{d+1} \sqrt{-g} \left( R - \frac{1}{2} \partial\Psi\partial\bar{\Psi} - V(\Psi\bar{\Psi}) \right), \quad (1.1)$$

where  $V$  is a scalar field potential, and  $\Psi \rightarrow e^{i\alpha}\Psi$  under the symmetry transformations. The latter symmetry allows for an interesting class of gravitational soliton-like solutions where the scalar field has a harmonic time dependence, with a nonetheless static stress-energy tensor, supporting the curved background metric on  $\mathcal{M}_{d+1}$ . Such configurations, named *boson stars*, were extensively studied in asymptotically Minkowski space-time [1] and in asymptotically AdS space-time beginning with the work [2]<sup>1</sup>.

Boson stars are expected to play an important role in holographic gauge theory/string theory correspondence [5]. Specifically, thermal states in microcanonical ensemble of strongly coupled four-dimensional conformal gauge theories (CFT) on  $S^3$  are represented by Schwarzschild (global)  $AdS_5$  black holes (BH), smeared over the compact manifold  $\mathcal{V}_5$  encoding the global symmetries of the CFT. This picture is correct for sufficiently large black holes in AdS (sufficiently energetic states in the CFT) [6]: as the BH gets smaller, it ultimately develops a Gregory-Laflamme instability [7] associated with its localization on  $\mathcal{V}_5$  [8–11]. The localization process corresponds to the

---

<sup>1</sup> The importance of boson stars for the AdS instability problem [3] was emphasized in [4].

dynamical spontaneous global symmetry breaking of the dual CFT. This suggests that supersymmetric conformal gauge theories on  $S^3$  can not have stable equilibrium states with unbroken  $R$ -symmetry below certain energy threshold. It was proposed in [12] that stable low-energy stationary states in  $R$ -symmetry singlet sector of conformal gauge theories are represented by boson stars in the gravitational dual.

Until now, the boson stars were discussed in the context of phenomenological gravity-scalar models. In this paper we construct boson stars in type IIB supergravity backgrounds holographically dual to strongly coupled quiver conformal gauge theories introduced in [13] (GHPT), and initiate analysis of their properties. Unlike the boson stars discussed earlier, boson stars arising in holography have local  $U(1)$  symmetry.

The rest of the paper is organized as follows. In the next section we review the correspondence between strongly coupled  $\mathcal{N} = 1$  superconformal gauge theories and holographically dual five-dimensional consistent truncations of type IIB supergravity introduced in [13]. We discuss in details the thermal equilibrium states in the theory with and without the condensate of the complex scalar field<sup>2</sup>. In section 3 we discuss boson stars in a toy model obtained from GHPT effective action removing the bulk gauge field (turning off the gauge coupling of the complex scalar field) and approximating the scalar potential with the appropriate mass term. We study boson stars in GHPT effective action in section 4. Finally, we conclude in section 5.

## 2 Quiver $\mathcal{N} = 1$ supersymmetric CFT holography

In this section we discuss the holographic correspondence between a large class of strongly coupled  $\mathcal{N} = 1$  superconformal quiver gauge theories and GHPT consistent truncation of type IIB supergravity on five-dimensional Sasaki-Einstein manifolds. We then study thermal equilibrium states within this consistent truncation.

### 2.1 GHPT effective action

At weak 't Hooft coupling, the gauge theory living on a world-volume of a large number  $N$  of D3-branes placed at the tip of a three complex dimensional Calabi-Yau cone  $X$  in type IIB supergravity is  $\mathcal{N} = 1$  superconformal (SCFT) quiver gauge theory with  $SU(N)$  gauge groups and a certain superpotential [14–17]. In the planar limit and

---

<sup>2</sup>In the former case we generalize the "holographic superconductor" transition for CFT on  $R^{3,1}$  in [13] to curved space-time,  $R \times S^3$ .

for large 't Hooft coupling the theory is best described by type IIB supergravity on  $AdS_5 \times Y_5$ , where the Einstein-Sasaki manifold  $Y_5$  is a level surface of  $X$ . Following [13] we consider examples where  $Y_5$  is expressible as a  $U(1)$  fibration over a compact Kähler-Einstein base. In this case the symmetry of the fiber geometrizes the  $R$ -symmetry of the SCFT.

Depending of which aspects of the dual gauge theories one wishes to study, one uses different consistent truncations of type IIB supergravity on  $AdS_5 \times Y_5$ . For example, to study the hydrodynamic transport in the theory [18] it is enough to consistently truncate to a five-dimensional gravity sector with a negative cosmological constant. Study of states of the theory with  $R$ -symmetry charge requires gauging the  $U(1)$  fiber isometry of  $Y_5$  [19]. Finally, to study boson stars in these SCFT one needs to enlarge the consistent truncation [19] to include a complex scalar field  $\Psi$ , charged under the  $R$ -symmetry. In a special case when  $\Psi$  is dual to a chiral primary operator  $\mathcal{O}_\Delta$  of a CFT with a scaling dimension  $\Delta = 3$  such a truncation was constructed in [13]. Explicitly, GHPT effective action takes form

$$S_{GHPT} = \frac{1}{16\pi G_5} \int_{\mathcal{M}_5} dx^5 \sqrt{-g} \left( R - \frac{L^2}{3} F_{\mu\nu} F^{\mu\nu} + \left( \frac{2L}{3} \right)^3 \frac{1}{4} \epsilon^{\lambda\mu\nu\sigma\rho} F_{\lambda\mu} F_{\nu\sigma} A_\rho - \frac{1}{2} \left[ (\partial\eta)^2 + \sinh^2 \eta (\partial_\mu \theta - q A_\mu)^2 - \frac{6}{L^2} \cosh^2 \frac{\eta}{2} (5 - \cosh \eta) \right] \right), \quad (2.1)$$

where  $\eta$  and  $\theta$  and the modulus and the phase of the complex scalar  $\Psi \equiv \eta e^{i\theta}$ , the five-dimensional Newtons constant is

$$G_5 = \frac{G_{10}}{\text{vol}(Y_5)}. \quad (2.2)$$

The  $R$ -charge of  $\Psi$ , dual to the chiral primary  $\mathcal{O}_3$ ,

$$| R[\Psi] | = q = \frac{2}{3} \Delta = 2, \quad (2.3)$$

is fixed by the superconformal algebra<sup>3</sup>. In what follows we set the asymptotic  $AdS_5$  radius  $L = 1$ . The ten-dimensional uplift of (2.1) can be found in [13].

## 2.2 Thermal state without scalar condensates in microcanonical ensemble

Consider thermal states in GHPT gauge theory plasma without the scalar condensate, *i.e.*,  $\eta = 0$ . These states are represented in a holographic dual by an electrically charged

---

<sup>3</sup>We use the standard normalization where the  $R$ -charge of the SCFT superpotential  $\mathcal{W}$  is  $R[\mathcal{W}] = 2$ .

(RN) black hole. We discuss RN black hole solution in some details mainly to set up our conventions.

We use the five-dimensional background metric as

$$ds_5^2 = \frac{1}{y} \left[ -ae^{-2\delta}(dt)^2 + \frac{(dy)^2}{4y(1-y)a} + (1-y)(d\Omega_3)^2 \right], \quad (2.4)$$

where  $(d\Omega_3)^2$  is a metric on a round  $S^3$  of unit radius, and  $\{a, \delta\}$  are the warp factors depending on the radial coordinate  $y$  varying from the AdS boundary  $y = 0$  to the location of the regular Schwarzschild horizon at  $y = y_0 < 1$ ,  $y \in [0, y_0]$ . The background further has a nontrivial bulk gauge potential

$$A = \phi(y) d(t). \quad (2.5)$$

Solving the equations of motion we find

$$\begin{aligned} \phi &= \frac{\mu(y_0 - y)}{y_0(1 - y)}, \quad \delta = 0, \\ a &= \frac{(y_0 - y)(y^2(4\mu^2 + 9)(y_0 - 1) - 18yy_0 + 9y + 9y_0)}{9(1 - y)^2y_0^2}. \end{aligned} \quad (2.6)$$

Following the AdS/CFT dictionary, the normalizable and the non-normalizable coefficients of various gravitational modes encode the CFT data. From a general AdS boundary expansion,

$$\phi = \mu + \phi_1^b y + \mathcal{O}(y^2), \quad a = 1 + a_2^b y^2 + \mathcal{O}(y^3). \quad (2.7)$$

$\mu$  is the RN black hole chemical potential, and the normalizable components

$$\phi_1^b = -\frac{\mu}{y_0} + \mu, \quad a_2^b = \frac{(y_0 - 1)(4\mu^2 y_0 + 9)}{9y_0^2}, \quad (2.8)$$

determine the charge  $Q$  and the mass  $M$  of RN black hole as

$$M = \frac{3}{4} \frac{\text{vol}(S^3)}{16\pi G_5} (1 - 4a_2^b), \quad Q = \frac{\text{vol}(S^3)}{2\pi G_5} \left( -\frac{1}{3}\phi_1^b \right). \quad (2.9)$$

Additionally, we can compute the temperature  $T$ , the entropy  $S$  and the grand potential  $\Omega$  of RN black hole as

$$\begin{aligned} (\pi T)^2 &= \frac{((4\mu^2 + 9)y_0 - 18)^2}{324y_0(1 - y_0)}, \quad ST = \frac{\text{vol}(S^3)}{16\pi G_5} \frac{2(1 - y_0)(18 - y_0(4\mu^2 + 9))}{9y_0^2}, \\ \Omega &= \frac{\text{vol}(S^3)}{16\pi G_5} \left( \frac{(5y_0 - 2)(2 - y_0)}{4y_0^2} - \frac{4(1 - y_0)}{9y_0} \mu^2 \right). \end{aligned} \quad (2.10)$$

Notice that the basic thermodynamic relations are satisfied:

$$\Omega = M - ST - \mu Q, \quad d(\Omega) = -S d(T) - Q d(\mu). \quad (2.11)$$

The vacuum of a SCFT is represent by global  $AdS_5$  solution,  $y_0 = 1$  and  $\mu = 0$ , in which case

$$M_{AdS_5} = \frac{3}{4} \frac{\text{vol}(S^3)}{16\pi G_5} \quad (2.12)$$

is the Casimir energy of the CFT ground state. In what follows we find it convenient to introduce the reduced mass  $\hat{M}$  and the charge  $\hat{Q}$  as follows

$$\hat{M} = \frac{M}{M_{AdS_5}} - 1, \quad \hat{Q} = \frac{2\pi G_5}{\text{vol}(S^3)} Q. \quad (2.13)$$

In a microcanonical ensemble, we keep the mass and the charge of a BH fixed, in which case we find

$$\hat{M}(\hat{Q}, y_0) = \frac{4(1 - y_0)}{y_0^2} + \frac{16y_0}{1 - y_0} \hat{Q}^2. \quad (2.14)$$

Notice that for a fixed  $\hat{Q}$ ,

$$\hat{M}(\hat{Q}, y_0) \geq \hat{M}_{min}(\hat{Q}) = 16 \hat{Q} + 16 \hat{Q}^2 - 32 \hat{Q}^3 + \mathcal{O}(\hat{Q}^4), \quad (2.15)$$

for small  $\hat{Q}$ ; for general  $\hat{Q}$ ,  $\hat{M}_{min}(\hat{Q})$  can be computed numerically.

In GHPT plasma, described holographically by (2.1), fixed charge equilibrium states (2.9), (2.10) become unstable with respect to the condensation of the complex scalar  $\Psi$  at low-energies — this is the "holographic superconductor" transition of [13] for a plasma in  $R^3$ . Similar phenomenon<sup>4</sup> occurs when GHPT plasma is confined on  $S^3$ . To determine the onset of the instability we linearize equation for<sup>5</sup>  $\eta(y) \equiv y^{3/2}\eta_1(y)$  (we can choose the gauge with  $\theta = 0$ ) on global RN black hole background (2.4)-(2.6). For

---

<sup>4</sup>We found that GHPT "superconducting" transition on  $R^3$  occurs at  $T = 0.0606766(2)\mu$ , in agreement with the result reported in [13].

<sup>5</sup>We explicitly factor the leading asymptotic behavior of  $\eta$  in defining  $\eta_1$ .

a fixed  $\hat{Q}$ , this equation takes form

$$\begin{aligned}
0 = & \eta_1'' + \left( 4y^2y_0^2(5y - 4y_0)\hat{Q}^2 + (y_0 - 1)(5y^3y_0 - 4y^2y_0^2 - 5y^3 - 4y^2y_0 + 6yy_0^2 + 4y^2 \right. \\
& \left. - 2y_0^2) \right) \left( 4y^3(-y_0 + y)y_0^2\hat{Q}^2 + y(y_0 - y)(1 - y_0)(y - 1)(yy_0 - y - y_0) \right)^{-1} \eta_1' \\
& + \left( 48y^3y_0^4(5y - 3y_0)\hat{Q}^4 + 12y_0^2(10y^4y_0^2 - 6y^3y_0^3 - 20y^4y_0 - 4y^3y_0^2 + 9y^2y_0^3 + 10y^4 \right. \\
& + 18y^3y_0 - 10y^2y_0^2 - 8y^3 - 2y^2y_0 + 6yy_0^2 - 3y_0^3)\hat{Q}^2 + 3(y_0 - 1)^2(y - 1)(yy_0 - y \\
& \left. - y_0)(5y^2y_0 - 3yy_0^2 - 5y^2 - 3yy_0 + 3y_0^2 + 3y) \right) \left( 64y^5y_0^4(-y_0 + y)\hat{Q}^4 + 32(y_0 - 1)(y \right. \\
& \left. - 1)(yy_0 - y - y_0)(y - y_0)y^3y_0^2\hat{Q}^2 + 4(y_0 - 1)^2(y - 1)^2(yy_0 - y - y_0)^2(y - y_0)y \right)^{-1} \eta_1.
\end{aligned} \tag{2.16}$$

Without loss of generality we can normalize  $\eta_1$  at the horizon to be one. Then, (2.16) has to be solved requiring normalizability of  $\eta$  (regularity of  $\eta_1$ ) at the  $AdS_5$  boundary

$$\eta_1 = \eta_{1,0} \left( 1 - \frac{9(4\hat{Q}^2y_0^2 - (y_0 - 1)^2)y}{8(y_0 - 1)^2} + \mathcal{O}(y^2) \right), \tag{2.17}$$

and regularity of  $\eta_1$  at the BH horizon

$$\eta_1 = 1 + \frac{3(8\hat{Q}^2y_0^3 + (2y_0 - 3)(y_0 - 1)^2)}{4(4\hat{Q}^2y_0^3 + (y_0 - 2)(y_0 - 1)^2)y_0} (y_0 - y) + \mathcal{O}((y_0 - y)^2). \tag{2.18}$$

Notice that given  $\hat{Q}$ , the regularity of the  $\eta_1(y)$  solution to the second order ODE (2.16) uniquely determines  $\{y_0, \eta_{1,0}\}$ . The obtained value of  $y_0$  can then we used in (2.14) to compute the mass of the RN black hole corresponding to the onset of the  $\Psi$ -condensation instability. The results of this analysis are presented in Figure 1. On the left panel, the solid black line corresponds to the mass  $\hat{M}_{crit}(\hat{Q})$  of the RN black hole below which it becomes unstable to developing  $\Psi$ -condensate. The dotted blue line represents the minimal mass of the RN black hole for a given  $\hat{Q}$ , see (2.15). On the right panel the solid black line represents the difference  $(\hat{M}_{crit}(\hat{Q}) - \hat{M}_{min}(\hat{Q}))$ .

### 2.3 Thermal states with scalar condensate in microcanonical ensemble

The end point of the RN BH instability in GHPT model, see (2.1), is a black hole with a nontrivial condensate of the complex scalar. We refer to it as RN- $\Psi$  black hole.

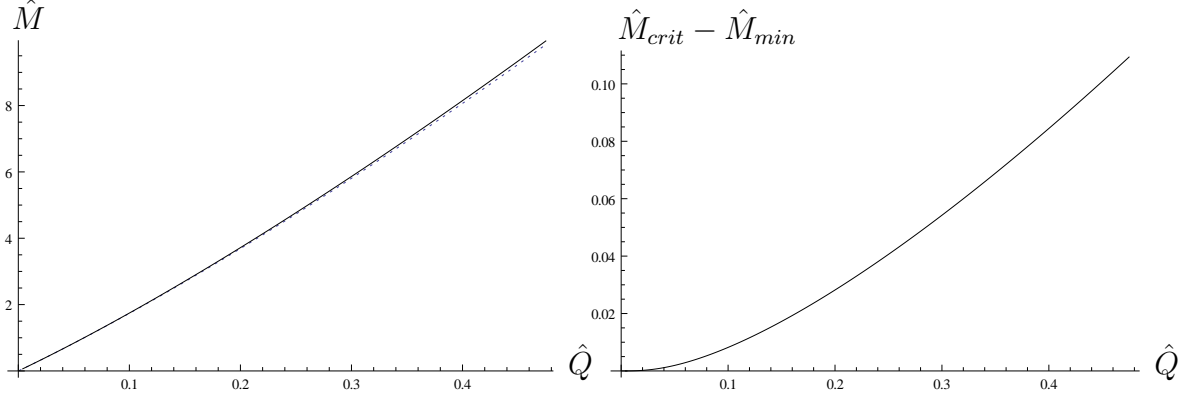


Figure 1: Left panel: Solid black line indicates the onset of the global  $AdS_5$  RN black hole instability with respect to developing a condensate of a charged scalar in GHPT model. The dotted blue line is the minimal mass of the RN BH for a given charge  $\hat{Q}$ , see (2.15). The RN black holes in a wedge between the blue and the black lines are unstable. This wedge is enlarged in the right panel.

Using the gauge  $\theta = 0$ , the background ansatz (2.4) and (2.5) supplemented with

$$c \equiv \cosh \eta = c(y), \quad (2.19)$$

we obtain the following equations of motion (in GHPT model  $q = 2$ ):

$$0 = a' + \frac{4}{9}(y-1)y^2 e^{2\delta} (\phi')^2 + \frac{(y-1)ay}{3(c^2-1)} (c')^2 - \frac{(c^2-1)q^2\phi^2}{12a} e^{2\delta} - \frac{(c-1)(c-3)}{4y} - \frac{(y-2)(a-1)}{y(y-1)}, \quad (2.20)$$

$$0 = \delta' + \frac{y(y-1)}{3(c^2-1)} (c')^2 - \frac{(c^2-1)q^2\phi^2}{12a^2} e^{2\delta}, \quad (2.21)$$

$$0 = c'' - \frac{c}{c^2-1} (c')^2 - \frac{4(y-1)y^2}{9a} e^{2\delta} c' (\phi')^2 + \frac{(c-2)^2(y-1) + a(8y-4) - 5y + 9}{4(y-1)ay} c' - \frac{cq^2\phi^2(c^2-1)}{4y(y-1)a^2} e^{2\delta} + \frac{3(c^2-1)(c-2)}{4a(y-1)y^2}, \quad (2.22)$$

$$0 = \phi'' - \frac{(y-1)y}{3(c^2-1)} \phi' (c')^2 + \frac{(c^2-1)q^2\phi^2}{12a^2} e^{2\delta} \phi' + \frac{2}{y-1} \phi' + \frac{3q^2(c^2-1)\phi}{16a(y-1)y^2}. \quad (2.23)$$



Equations (2.20)-(2.23) must be solved with the following asymptotic expansions:

- at the  $AdS_5$  boundary,  $y \rightarrow 0_+$ ,

$$\begin{aligned} a &= 1 + a_2^b y^2 + \left( \frac{4}{9}(\phi_1^b)^2 + c_3^b + a_2^b \right) y^3 + \mathcal{O}(y^4), & \delta &= \frac{1}{2}c_3^b y^3 + \mathcal{O}(y^4), \\ c &= 1 + c_3^b y^3 + \mathcal{O}(y^4), & \phi &= \mu + \phi_1^b y + \phi_1^b y^2 + \left( \phi_1^b + \frac{1}{4}\mu c_3^b \right) y^3 + \mathcal{O}(y^4); \end{aligned} \quad (2.24)$$

- at the regular Schwarzschild horizon,  $z \equiv y_0 - y \rightarrow 0_+$ ,

$$\begin{aligned} a &= \left( \frac{5 - (c_0^h - 2)^2}{4y_0} + \frac{4}{9}(y_0 - 1)y_0^2(d_0^h)^2(\phi_1^h)^2 + \frac{1}{y_0(1 - y_0)} \right) z + \mathcal{O}(z^2), \\ \delta &= \ln d_0^h + \frac{27(y_0 - 1)((c_0^h)^2 - 1)(16(d_0^h)^2(\phi_1^h)^2 y_0^3(1 - y_0) + 9(c_0^h - 2)^2)}{y_0(-16(d_0^h)^2(\phi_1^h)^2 y_0^3(1 - y_0)^2 + 9((c_0^h - 2)^2 - 5)(y_0 - 1) + 36)^2} z + \mathcal{O}(z^2), \\ c &= c_0^h + \frac{27((c_0^h)^2 - 1)(c_0^h - 2)}{y_0(-16(d_0^h)^2(\phi_1^h)^2 y_0^3(1 - y_0)^2 + 9((c_0^h - 2)^2 - 5)(y_0 - 1) + 36)} z + \mathcal{O}(z^2), \\ \phi &= \phi_1^h z + \mathcal{O}(z^2). \end{aligned} \quad (2.25)$$

Notice that given the non-normalizable coefficients  $\mu$  (the chemical potential) and the black hole size  $0 < y_0 < 1$ , the asymptotics of the solution are completely characterized by 6 parameters

$$\{\phi_1^b, a_2^b, c_3^b, d_0^h, c_0^h, \phi_1^h\}, \quad (2.26)$$

which is the correct number to uniquely specify the solution to a coupled system of 2 second-order equations (2.22), (2.23) and 2 first-order equations (2.20), (2.21):  $2 \times 2 + 2 \times 1 = 6$ . The mass and the charge of RN- $\Psi$  black hole are given as in (2.9) and (2.13)<sup>6</sup>:

$$\hat{M} = -4a_2^b, \quad \hat{Q} = -\frac{1}{3}\phi_1^b. \quad (2.27)$$

In a microcanonical ensemble it is appropriate to keep  $\hat{Q}$  fixed and construct a family of RN- $\Psi$  solutions parameterized by  $y_0$ . As the area of the BH horizon is given by

$$A_{horizon} = \frac{(1 - y_0)^{3/2}}{y_0^{3/2}} \text{vol}(S^3), \quad (2.28)$$

the limit  $y_0 \rightarrow 0$  corresponds to a vanishingly small BH. We use numerical techniques of [20] to construct families of RN- $\Psi$  black holes for different values of  $\hat{Q}$ . A typical family

---

<sup>6</sup>We also computed the remaining thermodynamic quantities in the grand canonical ensemble and verified the first law of thermodynamics (2.11) to an accuracy of better than  $10^{-6}$ .

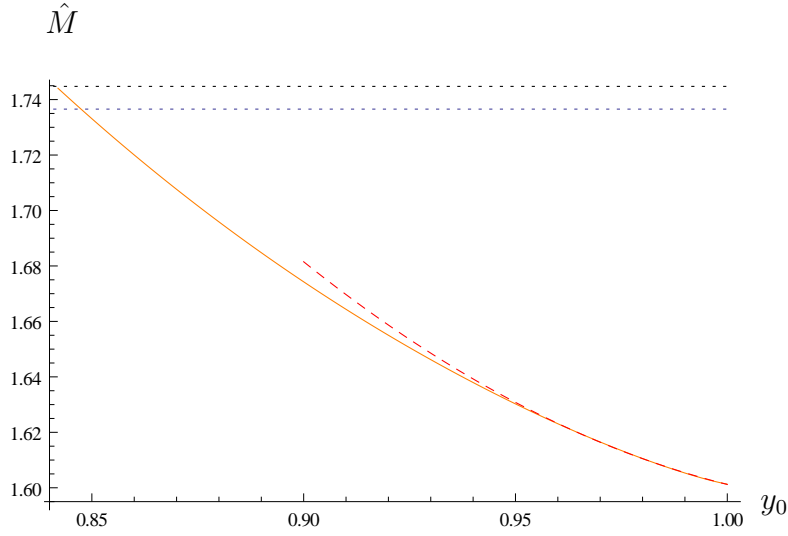


Figure 2: Solid orange line represents a family of RN- $\Psi$  black holes (charged black holes with nontrivial scalar hair) for a fixed  $\hat{Q} = 0.1$ . The dotted black line is the largest mass of the unstable RN black hole with this charge  $\hat{Q}$ , see (2.29). The dotted blue line is the smallest mass of the RN black hole with this charge  $\hat{Q}$ , see (2.30). The dashed red line is the best quadratic fit to the mass of small RN- $\Psi$  black holes, see (2.31).

(with  $\hat{Q} = 0.1$ ) is presented in Figure 2. The solid orange curve extends from  $y_0 = 0.842$  (the RN black hole becomes unstable at a slightly smaller value of  $y_0 = 0.841520144(9)$ ) to  $y_0 = 0.9999$  (the smallest black hole we studied). The dotted black line is the mass of the RN black hole at the onset of the  $\Psi$ -instability,

$$\hat{M}_{unstable} \Big|_{\hat{Q}=0.1} = 1.744761(0). \quad (2.29)$$

The dotted blue line represents the lightest RN black hole with the charge  $\hat{Q} = 0.1$ ,

$$\hat{M}_{min} \Big|_{\hat{Q}=0.1} = 1.736561(2). \quad (2.30)$$

The dashed red line is the best quadratic fit to the tail of the orange curve<sup>7</sup>,

$$\hat{M} \Big|_{red,dashed} = 1.601197(5) + 0.381186(8) (1 - y_0) + 4.219031(9) (1 - y_0)^2. \quad (2.31)$$

We would like to conclude this section with two observations:

---

<sup>7</sup>We use the last 50 data points,  $y_0 \in [0.959, 0.9999]$ .

- RN- $\Psi$  black holes can have a mass smaller than that of a minimal mass of a RN black hole for a given charge  $\hat{Q}$ ;
- in all examples we studied there is a bound on a minimal mass of RN- $\Psi$  black holes with a fixed charge, achieved when the corresponding black hole becomes vanishingly small; furthermore,

$$\min_{\hat{Q}=\text{const}} \left[ \hat{M}_{\text{RN-}\Psi} \right] > 16\hat{Q}. \quad (2.32)$$

### 3 Boson stars in a toy model

Setting  $q = 0$ , decoupling the bulk gauge field  $A_\mu = 0$ , and expanding GHPT effective action (2.1) to quadratic order in  $\eta$  we find

$$S_{\text{toy}} = \frac{1}{16\pi G_5} \int_{\mathcal{M}_5} dx^5 \sqrt{-g} \left( R + 12 - \frac{1}{2} \left[ (\partial\eta)^2 + \eta^2 (\partial\theta)^2 - 3\eta^2 \right] \right), \quad (3.1)$$

which is the effective action for the phenomenological boson stars (1.1) with

$$\Psi = \eta e^{i\theta}, \quad V(\Psi\bar{\Psi}) = -12 - \frac{3}{2}\Psi\bar{\Psi}. \quad (3.2)$$

Boson star solutions are found within the metric ansatz (2.4) supplemented with

$$\eta = \eta(y), \quad \theta = \omega t, \quad (3.3)$$

where  $\omega$  is a constant frequency of a boson star. Equations of motion and the asymptotic data from (3.1) take form

$$0 = a' + \frac{1}{3}ay(y-1)(\eta')^2 - \frac{\eta^2\omega^2 e^{2\delta}}{12a} - \frac{\eta^2(1-y) + 4(y-2)(a-1)}{4y(y-1)}, \quad (3.4)$$

$$0 = \delta' + \frac{1}{3}y(y-1)(\eta')^2 - \frac{\omega^2\eta^2 e^{2\delta}}{12a^2}, \quad (3.5)$$

$$0 = \eta'' + \frac{\eta^2(1-y) + 8ya - 4y - 4a + 8}{4ay(y-1)}\eta' - \frac{(e^{2\delta}\omega^2 y + 3a)\eta}{4(y-1)y^2 a^2}; \quad (3.6)$$

- at the  $AdS_5$  boundary,  $y \rightarrow 0_+$ ,

$$\begin{aligned} a &= 1 + a_2^b y^2 + \left( a_2^b + \frac{1}{2}(\eta_3^b)^2 \right) y^3 + \mathcal{O}(y^4), & \delta &= \frac{1}{4}(\eta_3^b)^2 y^3 + \mathcal{O}(y^4), \\ \eta &= y^{3/2} \left( \eta_3^b - \frac{1}{8}\eta_3^b(\omega^2 - 9) y + \mathcal{O}(y^2) \right); \end{aligned} \quad (3.7)$$

■ at the origin,  $z \equiv 1 - y \rightarrow 0_+$ ,

$$\begin{aligned} a &= 1 - \frac{1}{24}(\eta_0^h)^2((d_0^h)^2\omega^2 - 3)z + \mathcal{O}(z^2), & \delta &= \ln d_0^h - \frac{1}{12}(\eta_0^h)^2(d_0^h)^2\omega^2 z + \mathcal{O}(z^2), \\ \eta &= \eta_0^h - \frac{1}{8}\eta_0^h((d_0^h)^2\omega^2 + 3)z + \mathcal{O}(z^2). \end{aligned} \quad (3.8)$$

Effective action (3.1) has a global  $U(1)$  symmetry associated with  $\theta \rightarrow \theta + \alpha$ . The corresponding conserved current

$$J^\mu = -\frac{1}{4}\sqrt{-g}\eta^2\partial^\mu\theta, \quad \partial_\mu J^\mu = 0, \quad (3.9)$$

gives a charge density

$$\hat{Q} = -\frac{1}{4}\int_0^1 dy\sqrt{-g}\eta^2 g^{tt}\omega = \frac{1}{8}\int_0^1 dy\frac{(1-y)\omega\eta^2 e^\delta}{ay^2}, \quad (3.10)$$

where the overall normalization in (3.9) is fixed to agree with the  $\hat{M}$  – vs.  $-\hat{Q}$  curve for the ground state boson stars in supergravity in the limit  $\hat{Q} \rightarrow 0$ , see section 4. Since  $\hat{Q} \propto (\eta_3^b)^2 + \mathcal{O}((\eta_3^b)^4)$ , we can use  $\eta_3^b$  as a proxy for the boson star charge  $\hat{Q}$ ; then, for a fixed  $\eta_3^b$ , the asymptotics of the solution (3.7) and (3.8) are characterized by 4 parameters

$$\{\omega, a_2^b, \eta_0^h, d_0^h\}, \quad (3.11)$$

which is the overall order of the ODE system (3.4)-(3.6). The mass of a boson star is given by (2.9) and (2.13)

$$\hat{M} = -4a_2^b. \quad (3.12)$$

It is possible to construct analytic solutions to (3.4)-(3.6) perturbatively in the amplitude of  $\eta$ :

$$\begin{aligned} \eta(y) &= \sum_{n=0}^{\infty} l^{2n+1} \eta_{[2n+1]}(y), & a &= 1 + \sum_{n=1}^{\infty} l^{2n} a_{[2n]}(y), & \delta &= \sum_{n=1}^{\infty} l^{2n} \delta_{[2n]}(y) \\ \omega &= \sum_{n=0}^{\infty} l^{2n} \omega_{[2n]}, & \omega_{[2n]} &= \text{const}. \end{aligned} \quad (3.13)$$

To leading order we find:

$$\eta_{[1]} = \eta_{[1,j]} = (-1)^j {}_2F_1(-j, 3+j; 2, 1-y) y^{3/2}, \quad \omega_{[0]} = \omega_{[0,j]} = 3 + 2j, \quad (3.14)$$

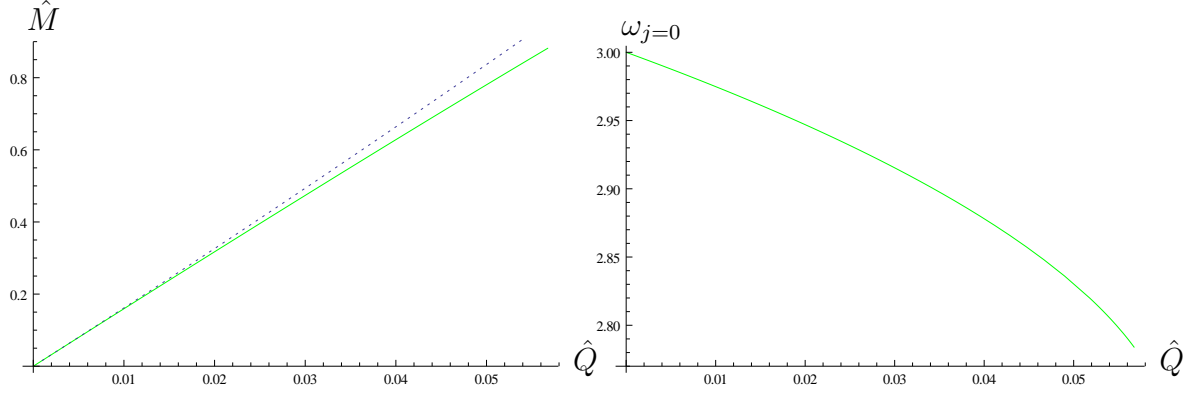


Figure 3: Left panel: The mass of the  $j = 0$  phenomenological boson star (solid green line), and the mass of the lightest RN black hole with the same charge (the dotted blue line). Right panel: frequency of the  $j = 0$  boson star.

where  $j = 0, 1, \dots$  is an index labeling different branches of boson star solutions. Furthermore, we find

$$\begin{aligned}\hat{Q} &= \hat{Q}_j = \frac{l^2}{8(j+1)(j+2)} + \mathcal{O}(l^4), \\ \hat{M} &= \hat{M}_j = \frac{2(3+2j)l^2}{3(j+1)(j+2)} + \mathcal{O}(l^4) = 16 \frac{\omega_j}{3} Q_j + \mathcal{O}(Q_j^2).\end{aligned}\tag{3.15}$$

Note that for a fixed  $\hat{Q}$ , higher  $j$ -level boson stars are more massive:

$$\hat{M}_{j+k}(\hat{Q}) > \hat{M}_j(\hat{Q}), \quad k = 1, 2, \dots.\tag{3.16}$$

Figure 3 represent numerical results for the  $j = 0$  phenomenological boson stars, fully nonlinear in  $\hat{Q}$ . Left panel: the solid green line represents the mass of the ground state boson stars as a function of the charge  $\hat{Q}$ . For reference, the dotted blue line is the mass of the lightest RN black hole (2.15) at the same charge. The right panel represents the ground state frequency of a boson star as a function of  $\hat{Q}$ .

Unlike black holes, boson stars do not exist<sup>8</sup> beyond some critical value of  $\eta_3^b$  (or corresponding the charge  $\hat{Q}$ ),

$$|\eta_3^b| \leq |\eta_{3,critical}^c| < 0.7887057630169999778594689006317396074408.\tag{3.17}$$

As Figure 4 demonstrates, there is no indication in the numerical results for (3.11) why there is a bound for  $\eta_3^b$ . Left panel presents results for  $a_2^b$  (blue curve) and  $\frac{\omega}{3}$  (black

<sup>8</sup>Similar phenomenon was observed in [2, 4, 12].

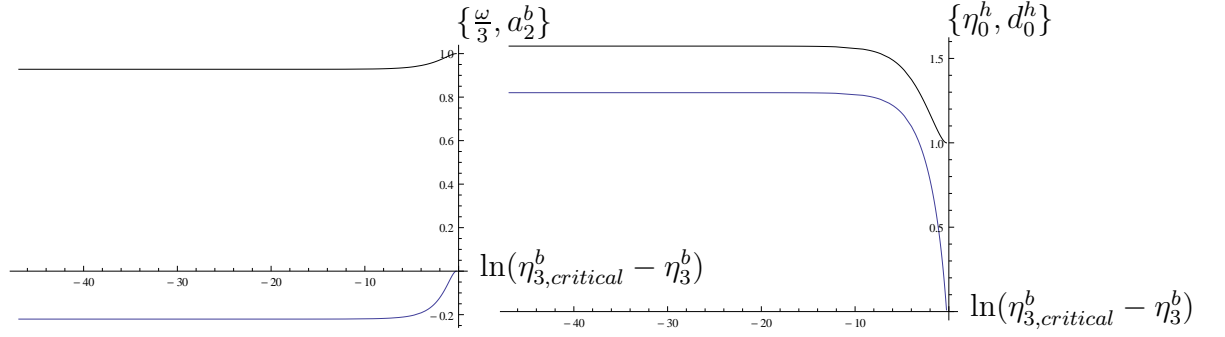


Figure 4: Dependence of the  $j = 0$  phenomenological boson star parameters (3.11) on  $\eta_3^b$ . Left panel:  $a_2^b$  (blue curve),  $\frac{\omega}{3}$  (black curve); right panel:  $\eta_0^b$  (blue curve),  $d_0^b$  (black curve). For  $\eta_{3,critical}^c$  we used the numerical upper limit as in (3.17).

curve) as a function of  $\eta_3^b$ . For  $\eta_{3,critical}^c$  we used the numerical upper limit as in (3.17). Right panel presents analogous results for  $\eta_0^b$  (blue curve) and  $d_0^b$  (black curve). It would be interesting to understand the physical reason for the existence of  $\eta_{3,critical}^b$  — previous linearized stability analysis of the phenomenological boson stars in [2, 12] found instabilities *prior to* reaching the analog of  $\eta_{3,critical}^b$ .

## 4 Boson stars in supergravity

To find boson stars in GHPT model (2.1) we use metric ansatz (2.4) along with

$$A = \phi(y) d(t), \quad c \equiv \cosh(\eta) = c(y), \quad \theta = \omega t. \quad (4.1)$$

The corresponding equations of motion are similar to (2.20)-(2.23) with the replacements

$$q^2 \phi^2 \rightarrow (q\phi - \omega)^2, \quad (4.2)$$

in all terms except for the last one in (2.23) where we replace

$$q^2 \phi \rightarrow q(q\phi - \omega)^2. \quad (4.3)$$

Type IIB supergravity embedding of GHPT model sets  $q = 2$ .

Asymptotic data for GHPT boson stars take form:

- at the  $AdS_5$  boundary,  $y \rightarrow 0_+$ ,

$$\begin{aligned}
a &= 1 + a_2^b y^2 + \left( a_2^b + \frac{4}{9}(\phi_1^b)^2 + c_3^b \right) y^3 + \mathcal{O}(y^4), & \delta &= \frac{1}{2}c_3^b y^3 + \mathcal{O}(y^4), \\
c &= 1 + c_3^b y^3 + \mathcal{O}(y^4), & \phi &= \phi_1^b y + \phi_1^b y^2 + \left( \phi_1^b - \frac{1}{16}q\omega c_3^b \right) y^3 + \mathcal{O}(y^4);
\end{aligned} \tag{4.4}$$

- at the origin,  $z \equiv 1 - y \rightarrow 0_+$ ,

$$\begin{aligned}
a &= 1 - \left( \frac{1}{24}(d_0^h)^2(\phi_0^h)^2((c_0^h)^2 - 1)q^2 - \frac{1}{12}(d_0^h)^2\omega\phi_0^h((c_0^h)^2 - 1)q + \frac{1}{24}(c_0^h - 1)(c_0^h(d_0^h)^2\omega^2 \right. \\
&\quad \left. + (d_0^h)^2\omega^2 + 3c_0^h - 9) \right) z + \mathcal{O}(z^2), \\
\delta &= \ln d_0^h - \frac{1}{12}(d_0^h)^2(\phi_0^h q - \omega)^2((c_0^h)^2 - 1) z + \mathcal{O}(z^2), \\
\phi &= \phi_0^h + \frac{3}{32}q((c_0^h)^2 - 1)(\phi_0^h q - \omega) z + \mathcal{O}(z^2), \\
c &= c_0^h - \frac{1}{8}((c_0^h)^2 - 1)(c_0^h(d_0^h)^2(\phi_0^h q - \omega)^2 - 3c_0^h + 6) z + \mathcal{O}(z^2).
\end{aligned} \tag{4.5}$$

The mass and the charge of the boson stars are given by (2.27). Note that for a fixed  $\hat{Q}$  (equivalently  $\phi_1^b$ ), the asymptotics of the solution are characterized by 6 parameters,

$$\{\omega, a_2^b, c_3^b, \phi_0^h, c_0^h, d_0^h\}, \tag{4.6}$$

which is the overall order of the coupled ODE system of the equations of motion.

As in section 3, we can construct boson stars perturbatively in the  $\eta(y)$  amplitude analytically. We have done it for the  $j = 0$  boson stars in GHPT model to order  $\mathcal{O}(l^{30})$  inclusive, where  $l$  is fixed as

$$c_3^b \equiv \frac{1}{2}l^2. \tag{4.7}$$

We find:

$$\begin{aligned}
\hat{Q}\Big|_{j=0} &= -\frac{1}{3}\phi_1^b \\
&= \frac{1}{16}l^2 + \frac{3}{256}l^4 + \frac{29}{5120}l^6 + \frac{8441}{2293760}l^8 + \frac{1903}{688128}l^{10} + \frac{68603543}{30277632000}l^{12} \\
&+ \frac{2357849941}{1199570944000}l^{14} + \frac{140271611444141}{78998944088064000}l^{16} + \frac{148011392983393047}{89532136633139200000}l^{18} \\
&+ \frac{28945266865118145121}{18371994437120163840000}l^{20} + \frac{45418739444730506807}{29692112221608345600000}l^{22} \\
&+ \frac{619893865521183402070738489}{411131694835982011465728000000}l^{24} + \frac{5303518796142734229022251479}{3523985955736988669706240000000}l^{26} \\
&+ \frac{9769477519044177078641271669913}{6435072951483980556753960960000000}l^{28} \\
&+ \frac{165805336474260222939581033601087896467}{107292400324955840088129241350144000000000}l^{30} + \mathcal{O}(l^{32}),
\end{aligned} \tag{4.8}$$

and, remarkably,

$$\omega\Big|_{j=0} = 3 + \mathcal{O}(l^{32}), \quad \hat{M}\Big|_{j=0} = 16 \hat{Q} + \mathcal{O}(l^{32}). \tag{4.9}$$

Turns out that relations (4.9) hold only for the ground state, *i.e.*,  $j = 0$ , and only for the supergravity value  $q = 2$ :

$$\begin{aligned}
\omega\Big|_{j=1} &= 5 + \left(-\frac{62}{105} + \frac{1}{28}q^2\right) l^2 + \left(-\frac{38170019869}{63567504000} - \frac{9328183}{9040711680}q^4\right) \\
&+ \frac{1871544527}{33902668800}q^2\Big) l^4 + \mathcal{O}(l^6) \\
\hat{M}\Big|_{j=1} &= \left(\frac{160}{3q} + \frac{4(15q^2 - 248)}{315q} \lambda^2\right) \hat{Q} + \mathcal{O}(l^4).
\end{aligned} \tag{4.10}$$

Precision fully nonlinear numerics confirmed that identities (4.9) are in fact exact.

As in case of the phenomenological boson stars discussed in section 3, here there is also a bound on  $c_3^b$ ; we find

$$c_3^b \leq c_{3,critical}^b < 0.43779161842835156074386507215849905168975. \tag{4.11}$$

Unlike phenomenological boson stars discussed in section 3, here we can understand



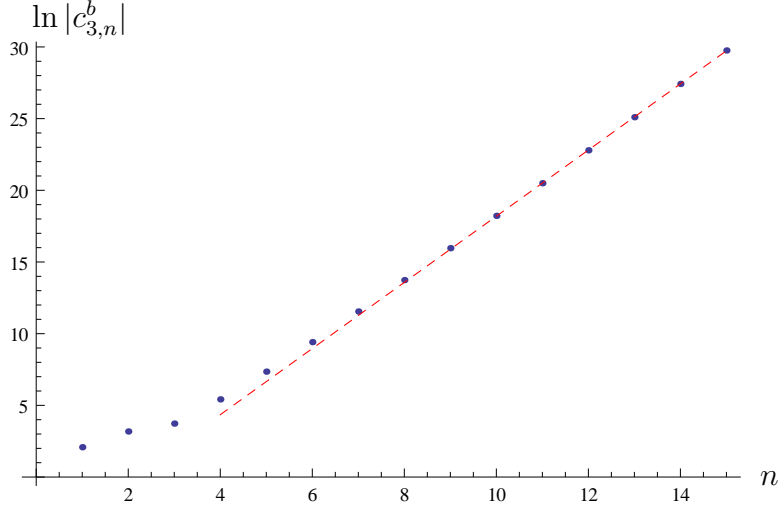


Figure 5: Perturbative expansion of  $c_3^b$  boson star parameter has a finite radius of convergence in  $\hat{Q}$ . The data points represent the first few expansion coefficients, see (4.12), and the red dashed line is the linear fit to the last five data points, see (4.13).

(at least at a technical level) the origin of  $c_{3,critical}^b$ . We can invert (4.8),

$$\begin{aligned}
c_3^b &= \sum_{n=1}^{\infty} c_{3,n}^b \hat{Q}^n \\
&= 8\hat{Q} - 24\hat{Q}^2 - \frac{208}{5}\hat{Q}^3 - \frac{7888}{35}\hat{Q}^4 - \frac{818176}{525}\hat{Q}^5 - \frac{352876624}{28875}\hat{Q}^6 - \frac{272007245344}{2627625}\hat{Q}^7 \\
&\quad - \frac{84964430758448}{91966875}\hat{Q}^8 - \frac{18253061040643088}{2131959375}\hat{Q}^9 - \frac{109122556608102498928}{1336738528125}\hat{Q}^{10} \\
&\quad - \frac{9101984161925699661824}{11436540740625}\hat{Q}^{11} - \frac{553801482686949813868971824}{70110393409546875}\hat{Q}^{12} \\
&\quad - \frac{61208627756373246966742061152}{769393278325546875}\hat{Q}^{13} - \frac{5249319592830812634726466094176}{6471955223561953125}\hat{Q}^{14} \\
&\quad - \frac{97973604596679544890714472505785440016}{11725726675168957623046875}\hat{Q}^{15} + \mathcal{O}(\hat{Q}^{16}).
\end{aligned} \tag{4.12}$$

Computed coefficients  $c_{3,n}^b$  are presented for  $n = 1, \dots, 15$  as blue dots in Figure 5. The dashed red line is the linear fit to the last five data points:

$$\ln |c_{3,n}^b| \Big|_{red,dashed} = -4.88369 + 2.30773 n. \tag{4.13}$$

The extracted asymptotic behavior of the coefficients  $c_{3,n}^b$  suggests that the radius of

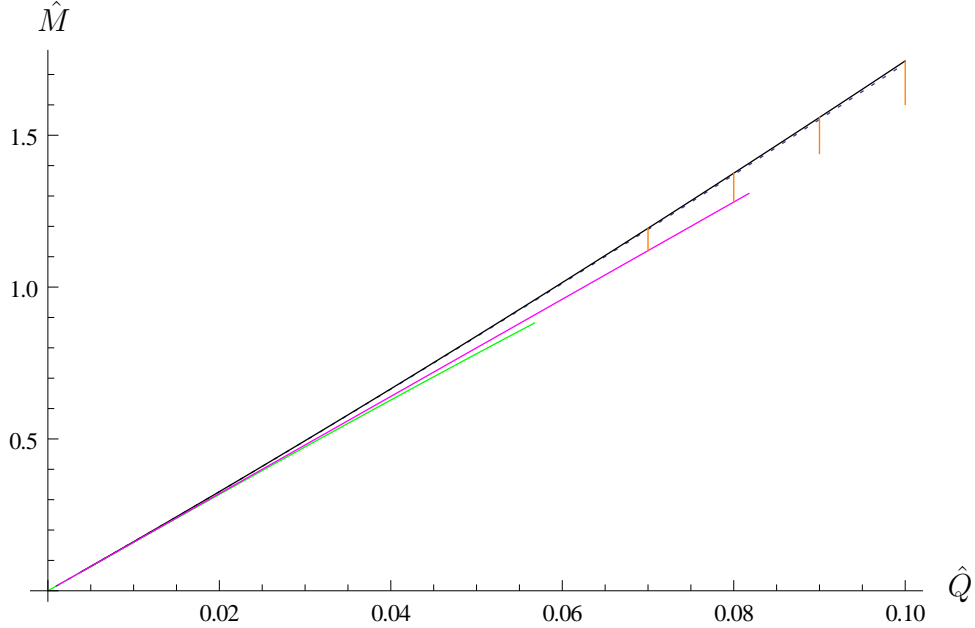


Figure 6: Charged states in GHPT model: the solid black curve represents RN black holes at the threshold of  $\Psi$ -condensation instability; dotted blue curve is the smallest mass RN black hole for a given charge  $\hat{Q}$ ; orange curves are RN- $\Psi$  black holes for select values of  $\hat{Q}$ ; the magenta line represents the ground state GHPT boson stars. The solid green curve represents ground state phenomenological boson stars.

convergence of the perturbative expansion (4.12) is

$$\hat{Q} \lesssim e^{-2.30773} = 0.0994864 \quad \implies \quad c_3^b \lesssim 0.395827, \quad (4.14)$$

corresponding to  $c_3^b$  bound close to (4.11).

Figure 6 collects the mass-charge dependence of various states in GHPT model. The solid black curve is the onset of the  $\Psi$ -scalar instability for RN black holes; the dotted blue curve is the smallest mass of the RN black hole for a given  $\hat{Q}$ . The orange curves represent the RN- $\Psi$  black holes (see section 2.3) for select values of  $\hat{Q}$ . They terminate (at low mass) as the RN- $\Psi$  black hole becomes vanishingly small. Our numerical results indicate that they terminate slightly above the magenta line, which represents the mass-charge relation for the ground state boson stars in GHPT:

$\hat{Q}$	min $\hat{M}$ [RN- $\Psi$ black hole]	$\hat{M}$ [ boson star]
0.07	1.120470(7)	1.12
0.08	1.280128(6)	1.28

Numerically, we can not access zero size RN- $\Psi$  black holes — it is possible that the precise  $y_0 \rightarrow 0$  limit of RN- $\Psi$  black holes saturates the  $\hat{M} = 16\hat{Q}$  relation of the  $j = 0$  boson stars. Finally, the solid green curve is the mass versus charge relation for the phenomenological  $j = 0$  boson stars discussed in section 3.

## 5 Conclusion

In this paper we studied boson stars — gravitational soliton-like configurations supported by a complex scalar field — in type IIB supergravity. More precisely, we focused on GHPT model [13], representing the holographic dual to a class of strongly coupled  $\mathcal{N} = 1$  quiver conformal gauge theories with a dimension  $\Delta = 3$  chiral primary operator  $\mathcal{O}_3$ . Earlier work [4, 12] indicated that boson stars (and boson-star-like configurations) play an important role in low-energy dynamics of holographic gauge theories, in particular regarding the question of equilibration. These earlier work (also [2]), however, were restricted to boson stars with global  $U(1)$  symmetry. In gravitational holographic duals to gauge theories the global symmetries must be gauged. The role of the corresponding local symmetry is played by  $R$ -symmetry in GHPT holography.

We studied in details the spectrum of charged states in GHPT plasma confined on  $S^3$  in a microcanonical ensemble. First, there are thermal states with  $\langle \mathcal{O}_3 \rangle = 0$ . These are represented by Reissner-Nordstrom (RN) black holes in global  $AdS_5$ . While important at high energy, these states are not expected to dominated the low-energy dynamics. On one hand, general arguments [6] suggest that they will be unstable<sup>9</sup> with respect to localization on a transverse compact space, spontaneously breaking the  $R$ -symmetry. In GHPT model there is a more mundane instability associated with developing the condensate  $\langle \mathcal{O}_3 \rangle \neq 0$  at sufficiently low energy for a fixed charge. These new states are thermal, and are represented by RN- $\Psi$  black holes. RN- $\Psi$  black holes reach below the mass threshold for the existence of RN black holes, almost (but not quite according to our numerics) reaching the ground state branch of the boson stars. The ground state GHPT boson stars represent remarkable configurations: unlike their counterparts in phenomenological models, their frequency is constant; furthermore, they saturate a BPS-like relation between the mass and the charge. However, these boson stars exist only below certain charge threshold.

We left many questions unanswered. It would be interesting to explicitly establish

---

<sup>9</sup>The instability was explicitly demonstrated only for neutral thermal states so far [8–11].

the GL instability of RN black holes following [11]. Likewise, it is important to establish the stability of GHPT boson stars, extending the work [12]. Is there a gap in the spectrum of RN- $\Psi$  black holes and the boson stars? Is it possible to construct charged initial conditions with energy less than that of a GHPT boson star? We hope to report on these questions in the future.

## Acknowledgments

I would like to thank Larry Yaffe for valuable discussions. Research at Perimeter Institute is supported by the Government of Canada through Industry Canada and by the Province of Ontario through the Ministry of Research & Innovation. This work was further supported by NSERC through the Discovery Grants program.

## References

- [1] S. L. Liebling and C. Palenzuela, “Dynamical Boson Stars,” *Living Rev. Rel.* **15**, 6 (2012) [arXiv:1202.5809 [gr-qc]].
- [2] D. Astefanesei and E. Radu, “Boson stars with negative cosmological constant,” *Nucl. Phys. B* **665**, 594 (2003) [gr-qc/0309131].
- [3] P. Bizon and A. Rostworowski, “On weakly turbulent instability of anti-de Sitter space,” *Phys. Rev. Lett.* **107**, 031102 (2011) [arXiv:1104.3702 [gr-qc]].
- [4] A. Buchel, S. L. Liebling and L. Lehner, “Boson stars in AdS spacetime,” *Phys. Rev. D* **87**, no. 12, 123006 (2013) [arXiv:1304.4166 [gr-qc]].
- [5] O. Aharony, S. S. Gubser, J. M. Maldacena, H. Ooguri and Y. Oz, “Large N field theories, string theory and gravity,” *Phys. Rept.* **323**, 183 (2000) [hep-th/9905111].
- [6] G. T. Horowitz, “Comments on black holes in string theory,” *Class. Quant. Grav.* **17**, 1107 (2000) [hep-th/9910082].
- [7] R. Gregory and R. Laflamme, “Black strings and p-branes are unstable,” *Phys. Rev. Lett.* **70**, 2837 (1993) [hep-th/9301052].
- [8] V. E. Hubeny and M. Rangamani, “Unstable horizons,” *JHEP* **0205**, 027 (2002) [hep-th/0202189].

- [9] O. J. C. Dias, J. E. Santos and B. Way, “Lumpy  $AdS_5 S^5$  black holes and black belts,” *JHEP* **1504**, 060 (2015) [arXiv:1501.06574 [hep-th]].
- [10] A. Buchel and L. Lehner, “Small black holes in  $AdS_5 \times S^5$ ,” *Class. Quant. Grav.* **32**, no. 14, 145003 (2015) [arXiv:1502.01574 [hep-th]].
- [11] A. Buchel, “Universality of small black hole instability in AdS/CFT,” arXiv:1509.07780 [hep-th].
- [12] A. Buchel and M. Buchel, “On stability of nonthermal states in strongly coupled gauge theories,” arXiv:1509.00774 [hep-th].
- [13] S. S. Gubser, C. P. Herzog, S. S. Pufu and T. Tesileanu, “Superconductors from Superstrings,” *Phys. Rev. Lett.* **103**, 141601 (2009) [arXiv:0907.3510 [hep-th]].
- [14] A. Kehagias, “New type IIB vacua and their F theory interpretation,” *Phys. Lett. B* **435**, 337 (1998) [hep-th/9805131].
- [15] I. R. Klebanov and E. Witten, “Superconformal field theory on three-branes at a Calabi-Yau singularity,” *Nucl. Phys. B* **536**, 199 (1998) [hep-th/9807080].
- [16] B. S. Acharya, J. M. Figueroa-O’Farrill, C. M. Hull and B. J. Spence, “Branes at conical singularities and holography,” *Adv. Theor. Math. Phys.* **2**, 1249 (1999) [hep-th/9808014].
- [17] D. R. Morrison and M. R. Plesser, “Nonspherical horizons. 1.,” *Adv. Theor. Math. Phys.* **3**, 1 (1999) [hep-th/9810201].
- [18] A. Buchel, R. C. Myers, M. F. Paulos and A. Sinha, “Universal holographic hydrodynamics at finite coupling,” *Phys. Lett. B* **669**, 364 (2008) [arXiv:0808.1837 [hep-th]].
- [19] A. Buchel and J. T. Liu, “Gauged supergravity from type IIB string theory on  $Y^{**p,q}$  manifolds,” *Nucl. Phys. B* **771**, 93 (2007) [hep-th/0608002].
- [20] O. Aharony, A. Buchel and P. Kerner, “The Black hole in the throat: Thermodynamics of strongly coupled cascading gauge theories,” *Phys. Rev. D* **76**, 086005 (2007) [arXiv:0706.1768 [hep-th]].